

# An Integrated Approach for Creating Model Diesel Fuels

Ioannis P. Androulakis,<sup>†</sup> Mark D. Weisel, Chang S. Hsu,<sup>‡</sup> Kuangnan Qian,  
Larry A. Green, and John T. Farrell\*

Corporate Strategic Research Laboratories, ExxonMobil Research and Engineering,  
1545 Route 22 East, Annandale, New Jersey 08801

Kiyomi Nakakita

Toyota Central Research and Development Laboratories, Inc., Nagakute,  
Aichi, 480-1192, Japan

Received April 27, 2004. Revised Manuscript Received September 24, 2004

This paper describes a methodology that has been developed to facilitate a detailed study of molecular composition effects on particulate matter emissions in advanced diesel engines. This includes a sophisticated numerical optimization algorithm to formulate well-characterized diesel fuel blends and an analytical method to characterize diesel fuels more accurately than previously possible. These tools are described, together with application to the formulation of test fuels with identical boiling point distribution and cetane number, but differing molecular composition. Test results are discussed from an advanced high-speed direct injection diesel engine for several of these fuels, demonstrating the improved insight and understanding available from these combined techniques.

## Introduction

Significant improvements in the efficiency and emissions of advanced internal combustion engines will require optimization of the entire fuel/engine/after-treatment system. There is growing recognition that the optimal fuel properties (i) are dependent on the engine operating conditions and (ii) can be different for different parts of the drive cycle. For example, highly aromatic, high-octane fuels have been shown to be optimal for operating high-compression-ratio gasoline engines at wide open throttle, while lower-aromatic, lower-octane fuels are optimal under low-load, stratified operation.<sup>1</sup> Understanding the effects of fuel composition at the molecular level promises to facilitate the identification of strategies to achieve maximum vehicle performance.

The study of fuel effects on emissions has a long history, and central to this has been the development of techniques to blend test fuels with desired properties. Historically, the fuel formulation was performed manually and was often time-consuming, tedious, and imprecise. Clearly, this approach can be (and was) best implemented when there is only a small number of targeted properties or blend components available. For example, a simple calculation shows that the number

of possible fuel combinations grows exponentially as the number of blend components increases. Furthermore, this approach is not readily amenable to characterizing the quality of the obtained solution, i.e., how well the actual blends meet the target values, because there is no way to determine the optimality using this type of selection. The advent of automated numerical methods has provided new opportunities for abandoning the “trial and error” approach in lieu of more-precise methods.

We report here the development of a numerical algorithm that facilitates the definition of model diesel fuels from well-characterized chemical streams. This approach possesses several key features:

- (i) It permits the cetane number (CN) of the fuels to be held approximately constant across the boiling point range;
- (ii) It allows a weighting factor to be applied to each of the target properties, so preference can be given to maximizing the fit to a specific property;
- (iii) It allows constraints to be imposed; and
- (iv) It minimizes the number of blend components.

Feature (iii) is, of course, necessary because it is not only desirable but usually essential to constrain parameters for the test fuels such as volatility range, ignition characteristics (octane or cetane number), elemental composition (sulfur, nitrogen), molecular composition (aromatics, olefins), vapor pressure, etc. More often than not, there are insufficient blend stocks to fully meet the design constraints, requiring compromises to be made.

While a computational algorithm as outlined previously permits the formulation of well-defined fuels, the quality of the agreement depends on accurate ana-

\* Author to whom correspondence should be addressed: E-mail: john.t.farrell@exxonmobil.com.

<sup>†</sup> Current address: Chemical & Biochemical Engineering Department, Rutgers, The State University of New Jersey, Piscataway, NJ 08854.

<sup>‡</sup> Current address: ExxonMobil Process Research Laboratories, Baton Rouge, LA 70821.

(1) Akihama, K.; Taki, M.; Takasu, S.; Ueda, T.; Iwashita, Y.; J. Farrell, T.; Weissman, W. Fuel Octane and Composition Effects on Efficiency and Emissions in a High Compression Ratio SIDI Engine. *SAE Tech. Pap. Ser.* 2004, 2004-01-1950.

Table 1. Definition of Z Numbers in the Current Study<sup>a</sup>

Z	identification
2(n)	<i>n</i> -paraffins
2(i)	isoparaffins
0	cycloparaffins
-2	dicycloparaffins
-4	tricycloparaffins
-6	benzenes
-8	indanes/tetralins
-10	dicyclobenzenes
-12	naphthalenes
-14	biphenyls/acenaphthenes
-16	fluorenes
-18	phenanthrenes

<sup>a</sup> Olefins are not included, because they are not present in the blend streams or fuels.

lytical characterization of the fuels. Although accurate analytical techniques have been developed for gasoline fuels, such techniques have been more difficult to develop for diesel fuels. It has proved particularly challenging to differentiate isoparaffins and cycloparaffins in complex mixtures such as diesel fuels, which readily undergo fragmentation upon conventional ionization in mass spectrometers to yield common fragment ions.

In this report, we describe the development of an analytical methodology for diesel fuel characterization that utilizes a combination of chromatographic and field ionization mass spectrometric techniques to provide the carbon number distribution for the following classes: *n*-paraffins, isoparaffins, cycloparaffins, and so on through the *z* numbers. The parameter *z* is given by  $C_nH_{2n+z}$  and reflects the degree of saturation of the molecule.<sup>2</sup> Table 1 provides identification of the various *z* numbers. Note that, strictly speaking, olefins and cycloparaffins share *z* numbers. For example, an olefin such as isobutene with a single unsaturated bond will have a *z* number of 0, as will a one-ring cycloparaffin such as cyclohexane. However, olefins are not present in either diesel fuel or the chemical streams used to blend the test fuels; therefore, we have omitted the corresponding olefin designations from Table 1 and the discussions that follow.

These two capabilities were developed as part of a study to discern the effects of fuel molecular structure on particulate matter (PM) emissions from high-speed direct-injection (HSDI) diesel engines. Well-characterized blends with precise compositional and physical targets were formulated with the numerical algorithm mentioned above, using analytical data generated with the analytical technique described below. Results from engine tests using these fuels are presented to demonstrate the capabilities of this approach and the detailed insight that can be derived from these detailed studies.

### Development of Numerical Algorithm for Formulating Model Fuel Blends

The formulation problem can be stated in a formal manner as follows: "Given a set of possible blending components from a list containing the analysis of each,

Table 2. Symbols Used in eq 1

symbol	definition
$\omega_j$	weighting factor for objective variable <i>j</i>
$\epsilon_j$	error of objective variable <i>j</i>
<i>T</i>	total number of points for boiling curve
$x_i$	mole fraction of component <i>i</i>
$BP_i(\tau)$	fraction of component <i>i</i> that has vaporized at temperature $\tau$
$TBP(\tau)$	target boiling point at temperature $\tau$
<i>P</i>	number of composition properties included in optimization
$CP_{i,j}$	value of property <i>i</i> in component <i>j</i>
$TP_i$	target property <i>i</i>
$y_i$	mass fraction of component <i>i</i>
$\rho_i$	density of component <i>i</i>
$\bar{\rho}$	target density
$CN_i$	cetane number of component <i>i</i>
$TCN_k$	target cetane number for boiling range <i>k</i>
<i>M</i>	variable that constrains threshold concentration of components in blend

determine a subset and their relative proportions, to meet a predefined set of target criteria". The *N* number of components from which the target fuels will be blended are characterized by a set of physical and chemical properties. The complete set of blending components will be hereafter denoted as the library. For the present study, the following parameters were chosen (additional properties can, of course, be added straightforwardly): (1) boiling curve, (2) normal paraffin content, (3) isoparaffin content, (4) one-ring cycloparaffin content, (5) two-ring cycloparaffin content, (6) multiring cycloparaffin content, (7) one-ring aromatics content, (8) two-ring aromatics content, (9), cetane number, and (10) density.

The problem to be solved involves identifying the subset of the *N* blend components, denoted  $N_c$ , that yields a fuel that meets the specifications defined by the set of target properties within the desired accuracy. The approach adopted is based on integer programming principles. The decision whether to include a particular component involves a logical decision, in which the existence/nonexistence of elementary units are modeled by the introduction of {0,1} variables. Each component of the library will thus be associated with a binary variable that takes the value 1 if the component is to be included in the final mixture, and 0 otherwise.

Two different sets of variables are defined. The variable  $x_i$  defines the mass or volume fraction of component *i* in the optimal blend. The variable  $\lambda_i$  defines a set of binary (i.e., {0,1}) variables that determine whether a particular component is included:  $\lambda_i = 1$  for components included in the blend, and  $\lambda_i = 0$  otherwise. These variables allow one to define all possible component combinations in a single mathematical formulation. The goal of the search is to determine how many  $\lambda_i$  are 1, i.e., which components are needed in the final mixture.

Although a larger  $N_c$  value typically yields closer agreement to target properties, the ideal solution will define the smallest number of components that are required to achieve the best approximation to the target fuel. Stated mathematically, the problem is best posed as a two-level optimization problem whereby one tries to maximize the ability of the blend to describe the properties of the real fuel, while utilizing the minimum number of components. The mathematical representa-

(2) Hsu, C. S.; Qian, K.; Chen, Y. C. An Innovative Approach to Data Analysis in Hydrocarbon Characterization by On-line Liquid Chromatography–Mass Spectrometry. *Anal. Chim. Acta* **1992**, *264*, 79–89.

tion of the problem is defined in eq 1:

$$\min_{\lambda_j, x_j} \sum_{j=1}^4 \omega_j \epsilon_j$$

subject to

$$\lambda_j \in \{0,1\}^{N_c}$$

$$x_j \in [0,1]^{N_c}$$

$$\sum_{t=1}^T \left\{ \frac{\sum_{\tau=1}^t \sum_{i=1}^{N_c} x_i \text{BP}_i(\tau) - \text{TBP}(\tau)}{\text{TBP}(\tau)} \right\}^2 \leq \epsilon_1$$

$$\sum_{i=1}^P \left\{ \frac{\sum_{j=1}^{N_c} x_j \text{CP}_{ij} - \text{TP}_i}{\text{TP}_i} \right\}^2 \leq \epsilon_2$$

$$\left\{ \frac{\sum_{i=1}^{N_c} y_i \rho_i - \bar{\rho}}{\bar{\rho}} \right\}^2 \leq \epsilon_3$$

$$\sum_{k=1}^4 \left\{ \frac{\sum_{i \in C_k} x_i \text{CN}_i - \text{TCN}_k}{\text{TCN}_k} \right\}^2 \leq \epsilon_4$$

$$y_i = \frac{x_i \rho_i}{\sum_{j=1}^{N_c} x_j \rho_j}$$

$$\sum_{i=1}^{N_c} x_i = N$$

$$x_i \leq \lambda_i \quad (\text{for } i = 1, \dots, N_c)$$

$$-Mx_i \leq -\lambda_i \quad (i = 1, \dots, N_c) \quad (1)$$

The symbols in eq 1 are defined in Table 2.

The fuel properties used to define the optimal blend include a root mean square (RMS) deviation of the integrated weight loss versus temperature (boiling point) curves of the target and blend fuels, the RMS deviation of the density between the target and the blend, and the RMS deviation of the remaining properties that blend volumetrically. The cetane number (CN) is treated separately and can be defined with respect to boiling range. The simplest treatment is to define the CN of only the final blend and allow the CN variation within the boiling range to be unconstrained. A defined (e.g., uniform) CN distribution across the boiling range can also be specified. This constraint is implemented by controlling the CN in four boiling-point regions that encompass the market diesel fuel range: very light (100–190 °C), light (165–250 °C), heavy (200–300 °C), and very heavy (>250 °C). Since each of the blend components is a chemical stream with fairly narrow boiling range, it is straightforward to assign them to one of these regions.

The formulation minimizes the deviation of the blend properties from the target properties by defining four so-called “slack” variables, which are the error variables denoted  $\epsilon$  in eq 1. Appropriate constraints are included: the sum of all volume fractions must equal one, and if a component is not selected, i.e.,  $\lambda_i = 0$ , its corresponding volume fraction must be zero, and vice versa. Minimizing the number of blended components simultaneously with the minimization of the slack variables is a multi-objective optimization problem. Because there is no clear way to penalize the increasing number of single components in the designed fuel, the problem is solved for increasing values of  $N_c$ . For a given value of  $N_c$ , the target of the optimization problem is thus to identify the  $N_c$  components and their fractions that minimize the error from the target fuel. The error, as a function of the number of blended components, is then reported. This allows a formulation to be chosen based on the optimal combination of both the error and the number of blended components.

The total solution to this problem belongs to the general and very difficult class of mixed-integer nonlinear problems (MINLP). The term “mixed” characterizes the fact that both continuous and binary variables are present in the formulation. One additional difficulty stems from the fact that this formulation is nonconvex and, therefore, additional effort must be invested to determine global solutions. The computational complexity is such that no general theory exists to solve this class of problem. There are several algorithmic details that are extremely important.<sup>3</sup> For example, the nonlinearities are due not only to the RMS error, but also to the densities, which blend on a mass basis, whereas the remaining components blend on a volume basis. The RMS nonlinearity can, in principle, be removed; however, definition of the densities introduced unavoidable nonlinearities.

For the solution of the MINLP problem, a Branch and Bound algorithm was used that partitions the space of the binary variables and successively sets these to their bounds. This is completed while solving the nonlinear continuous relaxation of the original MINLP, to determine valid upper bounds and eventually integer feasible solutions that correspond to optimal blends. The Branch and Bound algorithm defines a family of approaches used for the solution of problems that involve binary variables. The main objective is to perform an implicit enumeration of the alternatives (combinations of  $\lambda_i$  variables) without actually enumerating all of them. A key element in this process is the representation of the alternatives via a binary tree, as shown in Figure 1. Several blends simulating a variety of target refinery fuels were generated using this framework. A few sample results are presented in section 4 below to demonstrate the versatility and usefulness of the approach. Extrapolations to other cases would be fairly straightforward. No assumptions are made regarding the solution methodology; therefore, extending the approach is trivial and would simply require increasing the number of components or the extent of characterization in the library. Note that, in many respects, complete

(3) Floudas, C. A. *Nonlinear and Mixed-Integer Optimization: Fundamentals and Applications*; Oxford University Press: Oxford, U.K., 1995

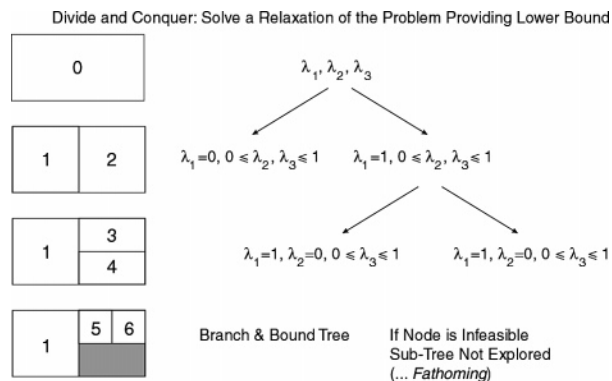


**Figure 1.** General structure of the binary tree used in the Branch & Bound algorithm to define fuel formulations subject to property constraints.

libraries make the search within this framework much easier. Unlike empirical approaches, one is not limited by one's ability to process a large number of data. Therefore, a larger number of blend components will improve the approximation and facilitate the convergence of the algorithm.

It is important to note that this approach can determine whether a target fuel can be formulated from the blend components while meeting the required tolerances or whether additional components are required. Furthermore, one can monitor the error contributions, to identify the chemical properties that are difficult to replicate. Therefore, one can readily identify the type of blend components that are needed to achieve the target values.

It is clear from our formulation that all properties are assumed to blend linearly with the volume or molar fraction. This assumption has been proven sufficiently valid to merit its use in this study. However, this assumption is easily relaxed in our model. The fundamental underlying algorithm simply addresses nonlinear problems and it is, therefore, up to the user to select an appropriate nonlinear mixing model.

### Analytical Methodology

The molecular compositions of petroleum middle distillates, including diesels, kerosenes, and jet fuels, are traditionally characterized in terms of hydrocarbon (compound) types (e.g., saturates, one-ring to three-ring aromatics) by a variety of chromatographic, mass spectrometry (MS), and combined chromatography/mass spectrometry methods.<sup>4–6</sup> Formal methods have been defined for the characterization of hydrocarbons in middle distillates using supercritical fluid chromatography (SFC) (ASTM Method D 5186) and liquid chromatography (e.g., IP 391).<sup>7</sup> These chromatographic

techniques provide a breakdown in total saturates and one-ring to three-ring aromatics but do not provide detailed quantitative information on compound-type distribution and carbon-number distribution within each compound type. Although MS methods such as ASTM Method D 2425 have been used for more-detailed hydrocarbon-type analyses, the approach requires careful calibration of the MS sensitivities (response factors) and does not yield carbon number distributions of the hydrocarbon types.

Gas chromatography–field ionization–time-of-flight mass spectrometry (GC–FI–TOF MS) is a new technology for hydrocarbon analysis.<sup>8</sup> In this technique, GC is used to separate hydrocarbon components by their boiling points. The accuracy and precision of the chromatographic retention times are better than 1 s. FI provides soft (low-energy) ionization of hydrocarbon molecules. Studies of model compounds<sup>9</sup> show that 3% or fewer of the molecules undergo fragmentation. Time-of-flight mass spectrometry (TOF-MS) resolves isobaric molecules (e.g., C/H<sub>12</sub> and C<sub>2</sub>H<sub>8</sub>/S doublets with  $\Delta M = 93.9$  and 90.5 mDa, respectively) through accurate mass measurement. Combined with GC separation, hard-to-resolve isobaric pairs such as C<sub>3</sub>/SH<sub>4</sub> ( $\Delta M = 3.4$  mDa), N/<sup>13</sup>CH ( $\Delta M = 8.2$  mDa) and O/CH<sub>4</sub> ( $\Delta M = 36.4$  mDa) can be completely or partially resolved. Such accurate and reproducible mass measurements (with an error of <3 mDa) thus permit determination of elemental compositions of the ions that serve as surrogates of the molecules.

The variation in ionization efficiency of molecules with varying structures and sizes makes quantitative analyses of petroleum by FI-MS challenging. In our work, quantification of GC–FI–TOF data is performed in two ways. First, response factors by carbon number (or molecular weight) are determined, using a mixture of alkyl benzene standard (C<sub>7</sub>–C<sub>25</sub>). Second, the total hydrocarbon classes, saturates, 1-ring aromatics, 2-ring aromatics, and 3+-ring aromatics are normalized to that determined by SFC. The resolution of isoparaffins versus normal paraffins and olefins versus cycloparaffins is based on chromatographic retention times.<sup>10</sup>

A schematic diagram of the GC–FI–TOF mass spectrometer is shown in Figure 2 and has been described previously.<sup>8</sup> The GC column is 30 m long (DB-1 HT) with 0.25  $\mu\text{m}$  film thickness and an inner diameter (ID) of 0.25 mm (J&W Scientific). The nonpolar nature of this column separates petroleum molecules by their boiling points. Approximately 1  $\mu\text{L}$  of the sample was injected via a Split/SplitLess (SSL) injector with a split ratio of 50:1. The temperature of the GC–TOF interface is maintained at 350 °C.

The details of FI-MS and TOF-MS can be found elsewhere.<sup>9</sup> In brief, the FI emitter consists of a 10- $\mu\text{m}$  tungsten wire onto which carbon dendrites (micro-

(4) Hsu, C. S. Diesel Fuel Analysis. In *Encyclopedia of Analytical Chemistry*; Wiley: New York, 2000; pp 6613–6622.

(5) Mendez, A.; Bruzual, J. Molecular Characterization of Petroleum and Its Fractionas by Mass Spectrometry. In *Analytical Advances for Hydrocarbon Research*; Hsu, C. S., ed.; Kluwer Academic/Plenum Publishers: New York, 2003; Chapter 4, pp 73–93.

(6) Aczel, T.; Hsu, C. S. Recent Advances in the Low Voltage Mass Spectrometric Analysis of Fossil Fuel Distillates. *Int. J. Mass Spectrom. Ion Phys.* **1989**, *92*, 1–7.

(7) Hsu, C. S.; Genowitz, M. W.; Dechert, G. J.; Abbott, D. J.; Barbour, R. Molecular Characterization of Diesel Fuels by Modern Analytical Techniques. In *Chemistry of Diesel Fuels*; Song, C., Hsu, C. S., Mochida, I., Eds.; Taylor & Francis: New York, 2000; Chapter 2, pp 61–76.

(8) Hsu, C. S.; Green, M. Fragment-Free Accurate Mass Measurement of Complex Mixture Components by Gas Chromatography/Field Ionization–Orthogonal Acceleration Time-of-Flight Mass Spectrometry: An Unprecedented Capability for Mixture Analysis. *Rapid Commun. Mass Spectrom.* **2001**, *15*, 236–239.

(9) Qian, K.; Dechert, G. J. Recent Advances in Petroleum Characterization by GC Field Ionization Time-of-Flight High-Resolution Mass Spectrometry. *Anal. Chem.* **2002**, *74* (16), 3977–3983.

(10) Qian, K.; Diehl, J. W.; Dechert, G. J.; DiSanzo, F. P. The Coupling of Supercritical Fluid Chromatography and Field Ionization Time-of-Flight High-Resolution Mass Spectrometry for Rapid and Quantitative Analysis of Petroleum Middle Distillates. *Eur. J. Mass Spectrom.* **2004**, *1*, 187–196.

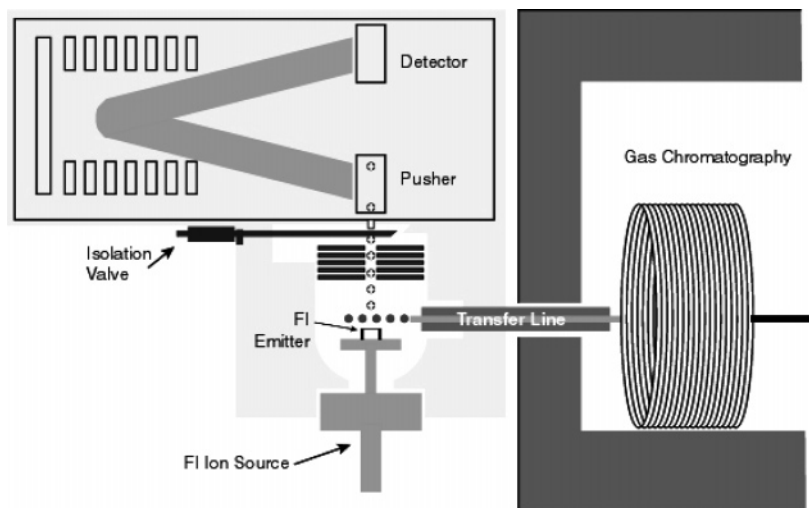


**Figure 2.** Schematic of the gas chromatography–field ionization–time-of-flight mass spectrometry (GC–FI–TOF MS) system utilized to characterize several of the chemical streams used to blend the test fuels.

needles) have been grown by “activation” in an organic vapor. The FI emitter is carefully aligned with the end of the GC capillary column so that the GC effluent passes near the tips of the carbon dendrites. The emitter (at ground voltage) is  $\sim 1.5$  mm away from a pair of extraction rods held at a high potential ( $-12$  kV), producing very high electric fields ( $\sim 10^7$ – $10^8$  V/cm) around the tips of the carbon dendrites. It is generally believed that, under a strong electric field, an electron can be removed from the molecule via quantum tunneling, generating molecular cations with minimal fragmentation.

Ions generated by FI were accelerated into a pusher region of the TOF mass analyzer. A 30-kHz, 960-V voltage pulse is applied orthogonally to the original ion path to direct the ions through a reflectron TOF with a total effective path length of 1.2 m. The reflectron geometry compensates for the energy differences of ions that have the same mass, thereby improving mass resolution. The ions are detected with a dual micro-channel plate with a clock rate of 3.6 GHz. A time-to-digital converter (TDC) translates the ion arrival time to molecular mass. The 30-kHz duty cycle leads to the generation of a full spectrum every 33  $\mu$ s and typically covers the mass range of 50–800 Da. The total spectrum accumulation is 1 s, corresponding to an accumulation of 30 000 spectra.

Calibration of the mass spectrometer was performed with a mixture of hydrocarbons covering the mass range of 50–800 Da. A typical calibration mixture contains heptacosafuorotributylamine, pentafluorobenzene, hexafluorobenzene, pentafluoriodobenzene, pentafluorochlorobenzene, perfluorotrimethylcyclohexane, xylene, and acetone. The mixture is introduced into the ion source via a batch inlet and is pumped out after the calibration. During sample analysis, a single lock-mass compound is introduced into the batch inlet and used as an internal reference for accurate mass measurement. In our experiments, pentafluoriodobenzene with a monoisotopic mass of 293.896 Da is used as the internal reference.

SFC analyses were based on a modified ASTM method.<sup>10</sup> A Hewlett-Packard model G1205A supercritical fluid chromatograph was configured with five SFC columns connected in series. An ES Industries 25 cm  $\times$

4.6 mm ID 60-Å Ring-Sep column (DNAP) was used to improve the separation between the one-ring and two-ring aromatics. The four Agilent Technologies 25 cm  $\times$  4.6 mm ID 5- $\mu$ m LichroSphere-SI60 silica columns in series improve the separation of the saturates and one-ring aromatics and effects a partial separation of the two- and three-ring aromatics. Carbon dioxide ( $\text{CO}_2$ ) is maintained isobarically at 2800 psi with a downstream backpressure control. The liquid  $\text{CO}_2$  flow rate is set at 2 mL/min. The SFC oven temperature is maintained at 31  $^\circ\text{C}$ . The injection volume of undiluted sample is 0.5  $\mu\text{L}$ .

Several of the components in the fuel blending library were pure components (decane, Decalin, and tetralin) and were not characterized as part of this study. The predominantly *n*-paraffinic streams were resolved and quantified via gas chromatography–flame ionization detection (GC–FID). All other chemical streams were characterized by GC–FI–TOF MS, with the exception of a family of highly branched multi-methyl paraffins. These streams, which have a chemical composition distinctly different from the isoparaffins in diesel derived from crude oil, exhibited significant fragmentation in GC–FI–TOF MS and were thus analyzed via GC–FID. It should be reiterated that the isoparaffins and cycloparaffins in crude-derived diesel undergo significantly less fragmentation upon FI, compared with the conventional ionization schemes using the established ASTM methods. Hence, the present methodology provides much more accurate compositional information for distillate streams. The only exception is the multi-methyl isoparaffinic stream that was mentioned previously. This difficulty is due to unusually high concentrations of molecules having tertiary branched structures, which differs significantly from the branching of isoparaffins present in petroleum-derived distillate streams. This high degree of branching results in facile fragmentation, even under mild FI conditions.

### Model Fuel Targets

The aforementioned techniques were used in a study to determine how molecular structures affect particulate matter (PM) emissions in a modern HSDI diesel engine. A fuel matrix was defined in which each fuel was

**Table 3. Target, Predicted (Model), and Actual (Experimentally Determined) Compositional Concentrations for Eight Test Fuels Formulated with the Approach Described in the Text**

	target	model	actual	target	model	actual	target	model	actual	target	model	actual
		TF-1			TF-2			TF-3			TF-4	
<i>n</i> -paraffins	0.40	0.37	0.40	0.40	0.32	0.35	0.40	0.37	0.35	0.40	0.39	0.40
isoparaffins	0.00	0.04	0.06	0.00	0.05	0.08	0.00	0.01	0.02	0.20	0.19	0.23
cycloparaffins												
1 ring	0.10	0.09	0.12	0.10	0.09	0.12	0.10	0.10	0.13	0.10	0.10	0.12
2+ rings	0.10	0.09	0.05	0.10	0.09	0.04	0.30	0.28	0.26	0.10	0.10	0.04
naphtho-aromatics	0.00	0.06	0.02	0.20	0.26	0.21	0.00	0.02	0.03	0.00	0.02	0.01
aromatics												
1 ring	0.20	0.17	0.17	0.20	0.17	0.18	0.20	0.21	0.19	0.20	0.19	0.18
2+ rings	0.20	0.18	0.17	0.00	0.02	0.01	0.00	0.02	0.02	0.00	0.02	0.02
number of components, $N_c$		10			7			7			8	
cetane number, CN	50	50	49	50	49	47	50	54	53	50	52	52
density, $\rho$	0.80	0.85	0.85	0.80	0.85	0.85	0.80	0.84	0.84	0.80	0.81	0.81
		TF-5			TF-6			TF-7			TF-8	
<i>n</i> -paraffins	0.40	0.35	0.35	0.40	0.42	0.43	0.40	0.39	0.39	0.80	0.75	0.75
isoparaffins	0.20	0.25	0.32	0.40	0.39	0.40	0.60	0.55	0.59	0.20	0.21	0.22
cycloparaffins												
1 ring	0.30	0.29	0.29	0.10	0.10	0.12	0.00	0.05	0.02	0.00	0.03	0.02
2+ rings	0.10	0.12	0.05	0.10	0.10	0.05	0.00	0.01	0.00	0.00	0.01	0.00
naphtho-aromatics	0.00	0.00	0.00	0.00	0.00	0.00	0.00	0.00	0.00	0.00	0.00	0.00
aromatics												
1 ring	0.00	0.00	0.00	0.00	0.00	0.00	0.00	0.00	0.00	0.00	0.00	0.00
2+ rings	0.00	0.00	0.00	0.00	0.00	0.00	0.00	0.00	0.00	0.00	0.00	0.00
number of components, $N_c$		6			10			5			8	
cetane number, CN	50	57	56	50	56	61	50	52	53	80	80	81
density, $\rho$	0.80	0.79	0.79	0.80	0.79	0.79	0.80	0.78	0.78	0.80	0.77	0.77

<sup>a</sup> The actual results are accurate to  $\sim 1\%$  (e.g.,  $0.40 \pm 0.01$ ).

targeted to have the same boiling point range (190–350 °C) and cetane number (53). The exception was the last fuel, which had a significantly higher targeted CN, as described below. In this study, the density slack variable was given a low weighting factor. Although density differences naturally exist between paraffins, naphthenes, and aromatics, these can be accounted for in the engine tests by varying the injection quantity to maintain equivalent fuel energy delivery. Density effects on spray (e.g., droplet densities) could not be separated from molecular class effects in our tests. The blend component library is comprised of 24 chemical streams, many of which (but not all) are primarily composed of a single class of molecules. For example, Norpar, Isopar, and Nappar commercial streams were included, which are composed primarily of *n*-paraffins, isoparaffins, and cycloparaffins, respectively. Similar streams for aromatics and naphtho-aromatics were included as well. Each of these chemical streams was subjected to the detailed analytical characterization described in the previous section, and the experimentally determined compositions were used in the fuel formulation.

The chemical composition and physical targets for the fuels are shown in Table 3. The first fuel is denoted TF-1 and has a composition that is effectively similar to current market diesel fuel, although with increased levels of 2-ring aromatics. The composition of the remaining fuels were determined based on hypothetical, idealized process steps. For example, TF-2 simulates the fuel that would result if all the 2+-ring aromatics were converted to tetralin-like structures through an idealized hydrotreating process. Similarly, fuel TF-3 simulates the fuel that would result if the tetralin-like structures of TF-2 were converted to 2+-ring naphthenes. TF-4 simulates the fuel that would result if the 2+-ring naphthenes underwent ring-opening to isoparaffins. The TF-5 fuel simulates TF-4 in which all the 1-ring aromatics have been converted to 1-ring naphthenes. TF-6 simulates TF-5 in which the 1-ring naphthenes have been ring-opened to isoparaffins. The TF-7

simulates TF-6 in which all the 1- and 2+-ring naphthenes are converted to isoparaffins. The final test fuel, TF-8, is a blend of isoparaffins and normal paraffins such as TF-7, except that the *n*-paraffin/isoparaffin ratio has been increased to yield a blend CN of 80. This blend was meant to simulate a Fischer–Tropsch diesel blend. Comparison to results from TF-7 would permit the determination of CN effects for fuels with very similar molecular composition. Figure 3 schematically illustrates the stepwise changes involved in these fuels.

It is important to note that the fuels are blended to targets defined by hypothetical processing steps. No actual processing is performed on the fuels. Rather, the fuels were blended from the chemical streams included in the library.

### Model Fuel Blends

The number of components ( $N_c$ ) required to meet the target properties for each fuel is given in Table 3 and ranges between 5 and 10. Figure 4 shows the decrease in error as a function of  $N_c$  for fuel TF-5, partitioned between the RMS deviation in the boiling point and other properties. Qualitatively similar results are obtained for all fuels. Table 3 shows the targeted chemical and physical properties, the predicted values based on the model, and the actual results determined from analytical characterization. Figure 5 shows the ASTM Method D-86 distillation curves for the eight test fuels, as well as for a “typical” diesel fuel, around which the boiling-point targets were largely based. It can be seen that many of the fuels deviate from the “typical diesel” curve over at least part of the range. The agreement could be improved only at the expense of decreasing the agreement with other properties, demonstrating the limitations imposed by the available blending library. Collectively, the data show that the target properties could be met with a reasonable number of blend components. Moreover, the agreement between the

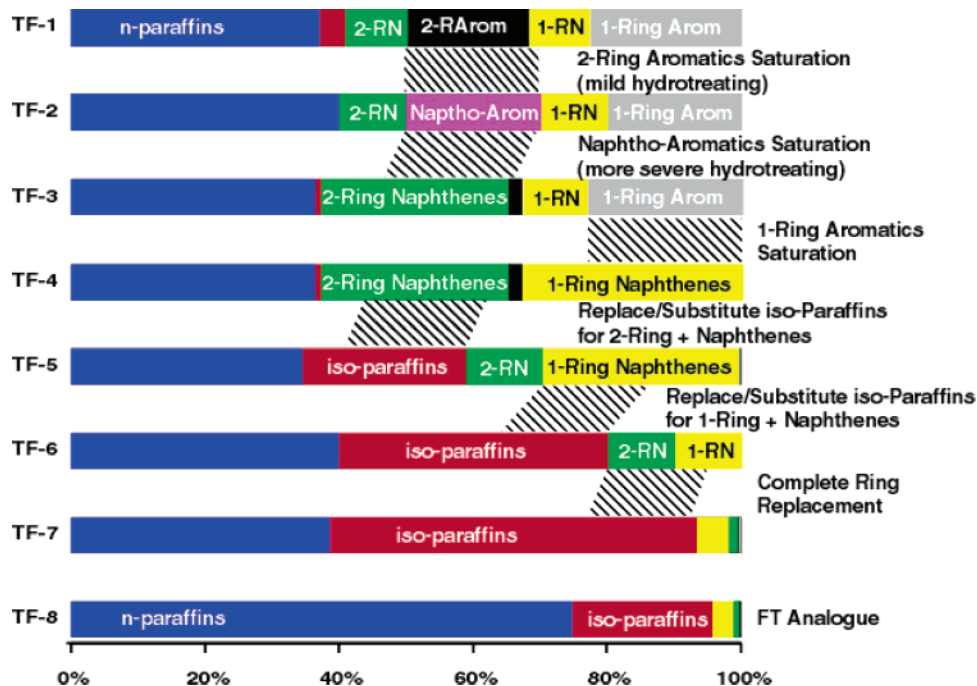


**Figure 3.** Molecular composition of matrix fuels formulated with numerical algorithm described in text. Also provided are descriptions of the simulated changes reflected in the compositional changes of each fuel (note that no actual processing of fuel streams occurred; see text for full details).

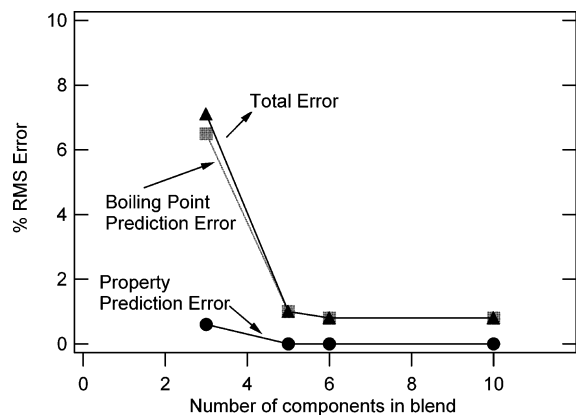


**Figure 4.** Percentage root mean square (RMS) error versus the number of blend components ( $N_c$ ) used to blend test fuel TF-5, showing that there is a critical number of components required to achieve the formulation targets.

model and actual results is quite good, demonstrating that the model and assumption of linear blending are adequate.

Figure 6 shows the carbon number distribution versus molecular class for TF-1, based on the analytical methodology used to characterize the blend components. Similar data were generated for all the test fuels. This graphical representation is useful not only to gauge the relative concentration of the various molecular classes, but also where they reside in the boiling-point range. For example, Figure 6 shows that the *n*-paraffins are concentrated in the front end of the boiling-point range, whereas the isoparaffins and cycloparaffins are concentrated in the back. These data can be extremely useful in understanding results from engine studies with these fuels.

### Single-Cylinder Engine Tests

Many studies have addressed the effects of diesel fuel properties on engine-out exhaust emissions (in particu-

lar, particulate matter (PM) formation).<sup>11–22</sup> Although it has been shown that fuel effects can vary, depending on the engine system, few studies have investigated the effects of fuel properties on in-cylinder processes such as fuel–air mixture formation, combustion, and chemical reaction processes. This information is essential to help determine the extent to which fuel properties contribute to PM formation. The present study focused on examining fuel effects in an engine in which the in-

(11) Ullman, T. L.; Mason, R. L.; Montalvo, D. A. Effects of Fuel Aromatics, Cetane Number, and Cetane Improver on Emissions from a 1991 Prototype Heavy-Duty Diesel Engine. *SAE Tech. Pap. Ser.* **1990**, 902171.

(12) Sienicki, E. J.; Jass, R. E.; W. Slodowske, J.; McCarthy, C. I.; Krodel, A. L. Diesel Fuel Aromatic and Cetane Number Effects on Combustion and Emissions from a Prototype 1991 Diesel Engine. *SAE Tech. Pap. Ser.* **1990**, 902172.

(13) Miyamoto, N.; Ogawa, H.; Shibuya, M.; Suda, T. Description of Diesel Emissions by Individual Fuel Properties. *SAE Tech. Pap. Ser.* **1992**, 922221.

(14) Arai, M. Impact of Changes in Fuel Properties and Lubrication Oil on Particulate Emissions and SOF. *SAE Tech. Pap. Ser.* **1992**, 920556.

(15) Kobayashi, S.; Nakajima, T.; Hori, M. Effect of Fuel Properties on Diesel Exhaust Emissions. *SAE Tech. Pap. Ser.* **1994**, 945121.

(16) Kobayashi, S.; Akiyama, K.; Nakajima, T.; Sasaki, S. Effect of Chemical Structure on Diesel Exhaust Emissions. *JSAE Paper No.* 9433588, 1994.

(17) Tsurutani, K.; Takei, Y.; Fujimoto, Y.; Matsudaira, J.; Kumamoto, M. The Effects of Fuel Properties and Oxygenates on Diesel Exhaust Emissions. *SAE Tech. Pap. Ser.* **1995**, 952349.

(18) Ogawa, T.; Araga, T.; Okada, M.; Fujimoto, Y. Fuel Effects on Particulate Emissions from DI Engine—Chemical Analysis and Characterization of Diesel Fuel. *SAE Tech. Pap. Ser.* **1995**, 952351.

(19) Akasaka, Y.; Sakurai, Y. Effects of Fuel Properties on Exhaust Emission from DI Diesel Engine. *Trans. JSME* **1997**, 63 (607), 1091–1097.

(20) Fujimoto, Y.; Tsukasaka, Y.; Takei, Y.; Nakada, M.; Ogawa, T. Effects of Diesel Fuel Properties on Particulate Emissions from DI Diesel Engine. In *Proceedings of the EAEC 5th International Congress*, SIA 9506A05, 1995.

(21) Hublin, M.; Gadd, P. G.; Hall, E. D.; Schindler, P. K. European Programmes on Emissions, Fuels and Engine Technologies (EPEFE)—Light Duty Diesel Study. *SAE Tech. Pap. Ser.* **1996**, 961073.

(22) Kwon, Y.; Mann, N.; Rieckard, J. D.; Haugland, R.; Ulvund, A. K.; Kvinge, F.; Wilson, G. Fuel Effects on Diesel Emissions—A New Understanding. *SAE Tech. Pap. Ser.* **2001**, 2001-01-3522.

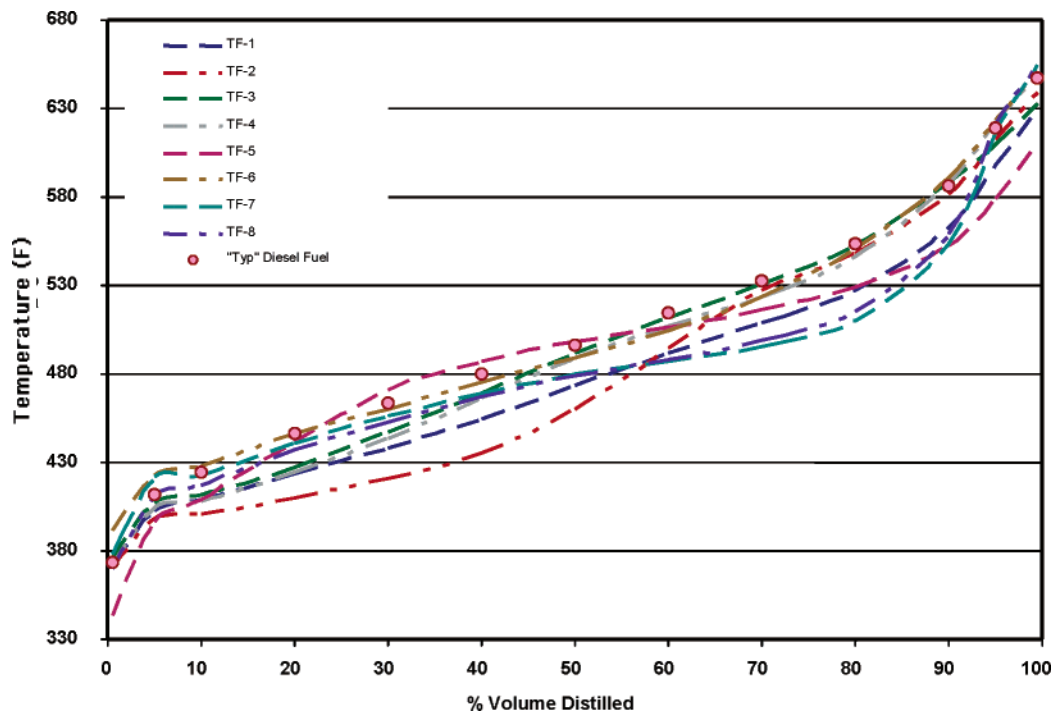


Figure 5. Distillation curve for all eight test fuels and reference diesel fuel.

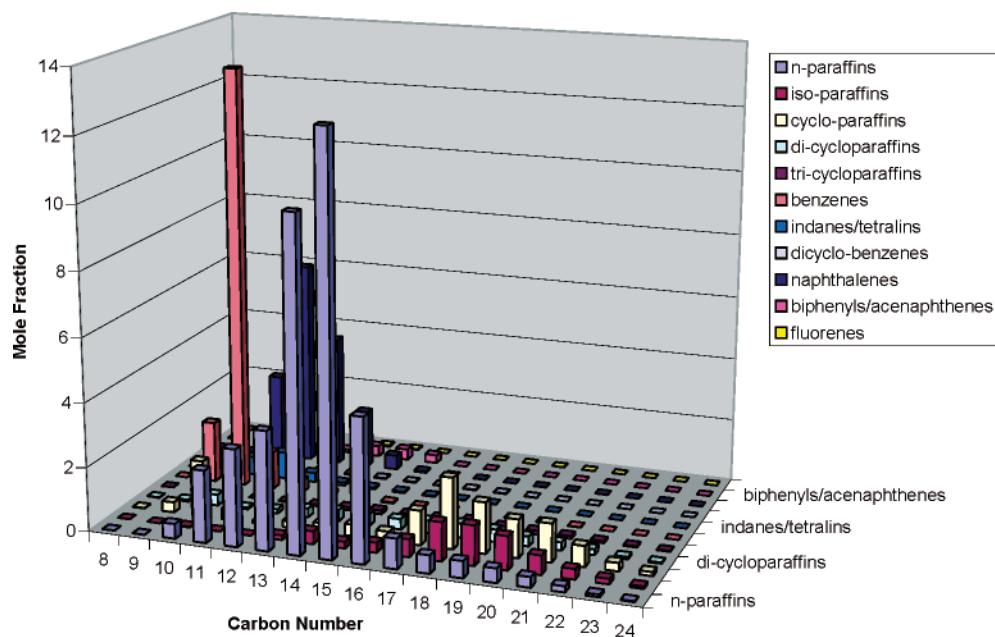


Figure 6. Carbon number versus molecular class for test fuel TF-1, based on the analytical characterization described in the text. The accuracy for each species from the mass spectrometric measurement is  $\sim 8\%$ .

cylinder fuel-air mixture formation was highly controlled and characterized. Full details are available elsewhere.<sup>23</sup>

Three types of single-cylinder HSDI diesel engines with modern combustion systems were used in this study, although only the results from the engine experiments directly pertinent to the present discussion will be outlined here. This involved a single naturally aspirated HSDI diesel engine with an electronically controlled, common-rail type, high-pressure fuel injection system.

Because of time constraints, results could not be obtained for all matrix fuels, and experimental data are only available for TF-1, TF-3, TF-5, TF-7, and TF-8. Exhaust emissions were measured under four fixed speed/load conditions that were representative of typical light-duty operating conditions. Combustion characteristics such as ignition delay, heat-release-rate pattern, and combustion periods were calculated via indicator analysis, based on the cylinder pressure and injector needle lift, which were recorded at a sampling rate of 0.5 crank angle degrees.

The PM emissions were measured at least three times at each operating condition, using a full-dilution tunnel, and the reported PM amount is the average of these. Exhaust after-treatment systems were not used, to

(23) Nakakita, K.; Ban, H.; Takasu, S.; Hotta, Y.; Inagaki, K.; Weissman, W.; Farrell, J. T. Effect of Hydrocarbon Molecular Structure in Diesel Fuel on In-Cylinder Soot Formation and Exhaust Emissions. *SAE Tech. Pap. Ser.* 2003, 2003-01-1914.

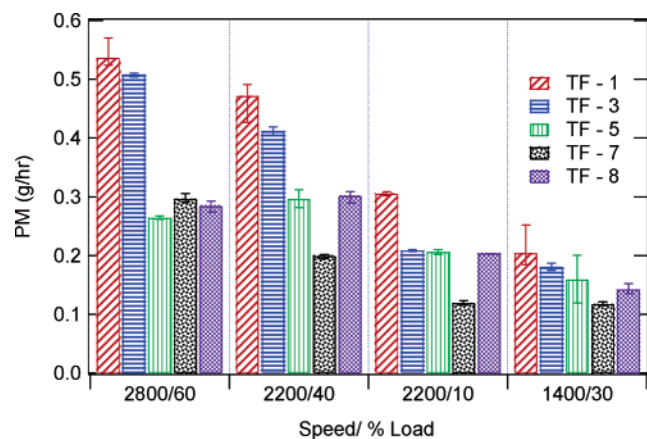


**Figure 7.** Engine-out exhaust particulate matter (PM) results from tests with several matrix fuels at four fixed speed/load conditions of an advanced, high-speed, direct injection (DI) diesel engine. Error bars represent an uncertainty of  $\pm 1\sigma$ , based on three repeat measurements. The precise control of the fuel formulation permits the differences in PM to be related to differences in fuel structure.

evaluate the fuel effects on engine-out emissions. The coolant and lubricant temperatures were kept constant at  $80 \pm 2$  °C.

The discussion that follows summarizes the PM emission results, which were the primary focus of the study. Other emissions (smoke, hydrocarbon, carbon monoxide (CO), and nitrogen oxides (NO<sub>x</sub>)) have been examined for these fuels as well, and the interested reader can consult ref 23 for more details.

The data for the TF fuels are shown in Figure 7. The figure shows that, under high load conditions (2800 rpm/60% load), PM emissions from the aromatics-containing fuels TF-1 and TF-3 are ~60%–70% higher than those from the paraffinic fuels TF-5, TF-7, and TF-8. TF-1 and TF-3 also yield higher PM emissions under the medium load test condition (2200 rpm, 40% load). The higher PM formation tendency of the aromatic fuels versus paraffinic fuels is consistent with many previous studies.<sup>17,19</sup> Under lighter-load/lower-speed conditions, the differences between the fuels diminishes when experimental uncertainty is considered. Among the paraffinic fuels, equivalent PM emissions are observed at high load and speed. Under medium- and light-load conditions, TF-7 gives significantly lower PM emissions. The highly *n*-paraffinic fuel TF-8 does not yield PM reductions that are as high as expected. This observation can be explained by the very high CN of TF-8 (CN = 80.5), which results in a significantly decreased ignition delay. Consequently, combustion is initiated before sufficient fuel–air mixing has occurred. Comparison of the PM emissions from TF-5 and TF-7 indicate that, at an almost equivalent CN, cycloparaffins (naphthenes) have a higher PM formation tendency than isoparaffins or *n*-paraffins. Generally, the effects of paraffin molecular structure on PM emission are large under medium- and low-load conditions, whereas they are much smaller under high-load conditions.

A detailed statistical analysis has been used to fit the PM data to equations that predict the mode PM emissions (in units of g/km) for a European driving cycle.<sup>23</sup> These equations include molecular composition variables. The general trends identified from this analysis are as follows: higher aromatics, naphthenes, PNA, CN,

and density all lead to increased PM. The magnitude of the coefficients in a statistical regression is commensurate with previous literature studies. A primary benefit of the current study is the ability to fit the data to a composition-based model. The results show that a fit to aromatics, naphthenes, and CN describes the data better than a conventional fit to aromatics, density, and CN. The latter approach often yields results difficult to interpret, because of the parameter correlation between aromatics and density. Moreover, a composition-based approach can provide the relative weighting of single-ring and multiring aromatics and naphthenes to PM formation and, thus, provides a straightforward means for considering modifications of the chemical composition of diesel fuels in such a way as to optimize the PM emissions. Expressing the fuel effects in chemical terms also allows well-to-wheel analyses of refining and vehicle impacts resulting from molecularly based fuel changes.

### Conclusions

Results have been presented for a program devised to discern the effects of fuel molecular structure on exhaust PM emissions in advanced high-speed direct-injection (HSDI) diesel engines. The program had three main components:

(1) Development of an optimization algorithm to blend well-characterized model diesel fuels from chemical streams.

(2) Development of accurate analytical characterization tools to accurately provide the carbon number distribution for various molecular classes.

(3) Experimental characterization in well-controlled engines of the effects of molecular structure.

The insight and understanding from component 3 was maximized by the successful implementation of components 1 and 2. A test matrix with fuels that have a carefully controlled chemical composition was prepared and analyzed, and a subset of these fuels was evaluated in a modern HSDI engine. Differences in particulate matter (PM) emissions were identified that are related to molecular structure. Statistical analysis of the results indicates that higher aromatics, naphthenes, PNA, cetane number (CN), and density all lead to increased PM. The best fit to the data is achieved with a composition-based model that includes CN, aromatics, and naphthene levels. Thus, this model is less subject to parameter correlation than traditional models that include density and provides information useful for investigating the impact of molecular-level changes in fuel composition on PM formation.

**Acknowledgment.** We gratefully acknowledge K. Akihama, Y. Takatori, M. Inayoshi, N. Mori, T. Takeshita, N. Shibayama, and Y. Esaki of Toyota Central R&D Labs., Inc., for their assistance to the experiments and for discussions. We would like to acknowledge A. M. Dean, J. Nishimura, D. J. Rikeard, C. H. Schleyer, and W. Weissman of ExxonMobil Research and Engineering for their assistance in performing these studies and for helpful discussions. In addition, we thank John W. Diehl and Frank P. DiSanzo for helping set up the SFC system and modified ASTM method. We also thank Gary Dechert for helping to conduct the GC-FI-TOF-MS analyses.

EF0498925